Surface morphology of SiO_2 coated InP/InGaAs/InGaAsP microstructures following the irradiation with ArF and KrF excimer lasers

Neng Liu, Khalid Moumanis, Jan J. Dubowski*
Laboratory for Quantum Semiconductors and Photon-based BioNanotechnology
Department of Electrical and Computer Engineering
Université de Sherbrooke, Québec, Canada J1K 2R1
*URL: http://www.dubowski.ca

ABSTRACT

Successful fabrication of devices from quantum well-intermixed material requires efficient control of its surface morphology. To address this problem, we have employed atomic force microscopy to study surface morphology of InP/InGaAs/InGaAsP QW microstructure coated with d_{SiO2} = 50, 150, 190, 243 and 263 nm thick SiO_2 films. Both ArF (193 nm) and KrF (248 nm) excimer lasers have been used to irradiate series of samples with up to 400 pulses of fluence 76 to 156 mJ/cm^2. The roughness (σ_{RMS}) of SiO_2 layer after both lasers irradiation and RTA decreases as the pulse number increases. Following RTA, a smoother surface morphology was observed for all irradiated samples. The cap InP layer was found to have a relatively smaller roughness (~ 0.4 nm) due to the protection provided by the SiO_2 layer during excimer laser irradiation and high temperature RTA. For samples coated with 50- or 150-nm-thick SiO_2 and irradiated by the ArF laser, the blueshift is only obtained when the SiO_2 layer was ablated. However, the sample coated with 243-nm-thick SiO_2 ($d_{SiO2} \approx \lambda_{KrF}$), following the 75-pulse-irradiation with the KrF laser at 124mJ/cm^2 and RTA, showed a smooth surface (σ_{RMS} = 1.8 nm) and maximum blueshift of 74 nm achieved without removal of the SiO_2 layer.

Keywords: Surface morphology, Quantum Well Intermixing, InP/InGaAs/InGaAsP microstructure, ArF excimer laser, KrF excimer laser, blueshift, SiO_2 layer, photonic devices

1. INTRODUCTION

Post growth quantum well intermixing (QWI) is an attractive method to engineer the bandgap of quantum well (QW) semiconductors. It allows active and passive components to be integrated monolithically at relatively reduced costs.[1] Various QWI techniques have been developed, including impurity free vacancy intermixing,[2] impurity induced intermixing,[3] plasma assisted intermixing[4] and laser induced intermixing.[5] Excimer laser irradiation on III-V semiconductors surfaces has been investigated for this purpose due to its simplicity in achieving selected area bandgap engineering of GaAs[6] and InP based QW microstructure.[7]

Impurity free vacancy disordering technique has been investigated, where a SiO_2 layer deposited on top of InP based multiple quantum well (MQW) and quantum dot (QD) microstructures was used to facilitate intermixing through In and Ga atom outdiffusion,[8] or efficient creation of group V interstitials that promote intermixing during rapid thermal annealing (RTA).[9] However, in continuous wavelength (CW) Nd:YAG laser RTA, group V atoms outdiffuse reaching SiO_2 layer through microcracks created during laser processing which enhance the As/P intermixing in InAs/InP QD microstructure.[10]

Due to the relatively low thermal and chemical stability of III-V compound semiconductors, laser irradiation can alter the structural, optical and electronic properties of these materials.[11] For instance, it was reported that the Atomic Force

Laser Applications in Microelectronic and Optoelectronic Manufacturing (LAMOM) XVI,
edited by Bo Gu, Guido Hennig, Xianfan Xu, Hiroyuki Niino, Proc. of SPIE Vol. 7920,
79200C · © 2011 SPIE · CCC code: 0277-786X/11/$18 · doi: 10.1117/12.879453

Downloaded from SPIE Digital Library on 03 Dec 2011 to 70.52.100.151. Terms of Use: http://spiedl.org/terms

Microscopy (AFM) measured surface roughness of InP irradiated by a nanosecond UV laser (λ=337 nm) increases systematically with the laser pulse number.[12] However, the InP surface crystalline structure and chemical composition remain unchanged for up to 6000 pulses of the below-ablation threshold fluence. At higher pulse fluences, nanosecond lasers are reported to decompose thermally InP and lead to a preferential removal of phosphorous.[13]

It is well known that SiO_2 layer is relatively transparent to ArF and KrF excimer laser wavelengths,[14] and it has been shown that KrF laser irradiation of a SiO_2 coated Si wafer can melt Si and create a periodic surface structure, without removal of the SiO_2 layer.[15] However, the cross sectional SEM micrographs show that some Si protrudes the SiO_2 layer and, thus, a modified interface profile is observed.[16] Simulation of laser interaction with SiO_2 coated materials indicates that the SiO_2 layer can be melted or ablated if the laser fluence is large or the substrate adjacent to the SiO_2 layer has a large absorption at this wavelength.[17]

In this study, we used both ArF and KrF lasers to irradiate InGaAs/InGaAsP microstructures coated with InP and different thickness SiO_2 layers. The surface morphology of SiO_2 and InP layers was examined with AFM after both laser irradiation and RTA.

2. EXPERIMENT

A schematic cross-section of the investigated QW structure is shown in Figure 1. It consists of 5 6-nm-thick $In_{0.47}Ga_{0.53}As$ wells separated by 4 10-nm-thick $In_{0.74}Ga_{0.26}As_{0.57}P_{0.43}$ barriers. The QW structure is grown on n-doped InP substrate and is designed to emit at 1.540 μm at room temperature. Samples, typically 8 mm x 8 mm, were first cleaved from a wafer and cleaned with standard solvents. Layers of SiO_2, d_{SiO2}= 50, 150, 190, 243, and 263 nm thick were deposited on top of the QW structure by a plasma enhanced chemical vapour deposition (PECVD) method. The SiO_2 films had their extinction ratio of 10^{-7} at the incident wavelength of 632.8 nm.

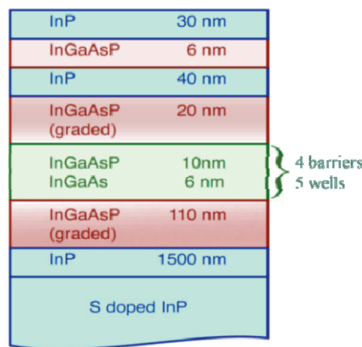

Figure 1. Schematic cross-section of the investigated QW structure.

We used an ArF laser (λ=193nm) delivering 16 ns pulses of fluence in the range of 67-150 mJ/cm^2, and a KrF (λ=248 nm) laser delivering 23 ns pulses of fluence in the range of 100-190 mJ/cm^2. Double microlens fly-eye-array homogenized laser beams were used to project a circular mask on the sample surface. With computer controlled X-Y-Z-Theta sample stages, the two setups allowed for the processing of samples at different sites of approximately 0.9 and 1.4 mm in diameter for ArF and KrF laser, respectively. The irradiation was carried out in an ambient air environment.

Following the irradiation, the sample was annealed with a commercial RTA processor (Jetfirst) in an atmosphere of mixed hydrogen and nitrogen (0.1: 0.9) at 700° C for 2 minutes. Thus, the annealing conditions for different sites on the same sample were nominally the same. After RTA, the SiO_2 layer was removed by immersing the whole sample in a 10% solution of HF in deionized H_2O.[18]

Room temperature photoluminescence (PL) measurements were carried out with a commercial mapper (Philips PLM-150). A Nd:YAG laser was used to excite the sample while the luminescence was dispersed by a monochromator and detected by an InGaAs photodiode array. The PL maps were obtained based on the QW electron-hole recombination peak, which for the as-grown material was located at 1540 nm.

Sample surface morphology was imaged with an Atomic Force Microscope (AFM) (Digital Instrument, Nanoscope III) operating in a tapping mode. An etched single-crystal silicon tip with a rectangular, single beam cantilever TESP (Digital Instruments) was used for collecting AFM images. The TESP tip radius is around 5-20 nm, the cantilever spring constant

Downloaded from SPIE Digital Library on 03 Dec 2011 to 70.52.100.151. Terms of Use: http://spiedl.org/terms

is 20-100 N/m and the resonance frequency is around 200-400 kHz. The tapping mode images were collected at scan rate of 1.97 Hz for 5 µm x 5 µm region and at 1.45 Hz for 2.5 µm x 2.5 µm, or smaller region, (512 points per line), which is reported to have higher accuracy in roughness measurements.[19] The root mean square surface roughness, σ_{RMS}, of the investigated samples was determined as the standard deviation of Z in the given region:[20]

$$\sigma_{RMS} = \sqrt{\frac{\sum_{i=1}^{N}(Z_i - Z_{av})^2}{N}}$$

where Z_{av} is the average Z value in this region, Z_i is the i-th Z value, N is the point within this region.

A commercial profilometer (Tencore alphastep 200) has been used to measure the ablation depth of the laser irradiated sites.

3. RESULTS AND DISCUSSIONS

3.1 ArF laser induced QWI on samples coated with SiO_2 layer

The bandgap energy of SiO_2 (9 eV) is greater than photon energy of both ArF (~6.4 eV) and KrF (~5.0 eV) lasers.[21] Hence, the SiO_2 layer should absorb only weakly the radiation of these lasers.[14] Figure 2 shows PL maps of samples coated with 50 and 150 nm thick SiO_2 layers that were irradiated with the ArF laser at pulse fluence of 76 mJ/cm^2. PL maps and microscope images are shown in top and bottom rows of each series. It can be seen that SiO_2 layers were not ablated completely, even with 400 pulses. Also, the results indicate that an obvious blueshift takes place only in the regions where the SiO_2 layer is ablated. This suggests that for the investigated 50 and 150 nm thick SiO_2 layers, the ArF radiation is not efficient to generate defects in the InP layer that would promote the intermixing process.

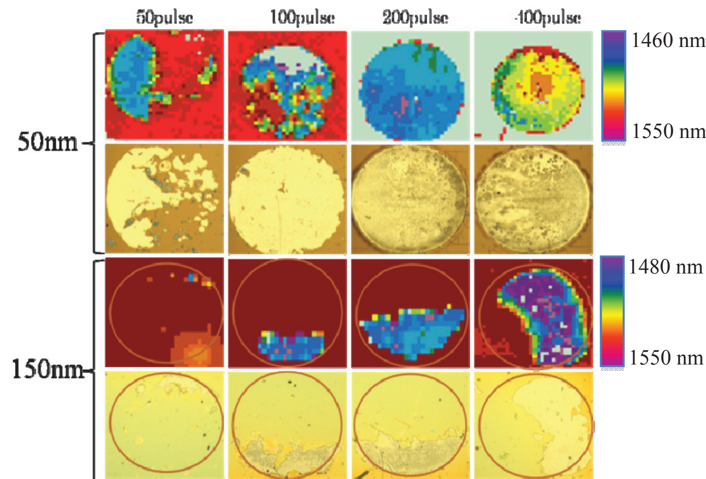

Figure 2. Room temperature PL maps and microscopic pictures of a series of spots on SiO_2 (50 and 150 nm thick) coated QW microstructures irradiated with ArF laser at 76 mJ/cm^2.

Figure 3 shows 2.5 µm x 2.5 µm 2D AFM images of the as-grown, 150 nm thick, SiO_2 layer (Fig. 3a), and after it was irradiated with 20 (Fig. 3b) and 100 pulses (Fig. 3c) of the ArF laser. In each case, the as-grown and laser irradiated samples were RTA for 2 min at 700° C. One notices that the laser-irradiated sites have, qualitatively, similar grain structure as that of the as-grown material. The grain structure is formed during PECVD,[22] with the grain size depending on the SiO_2 layer thickness.[23] The corresponding cross-section profiles, shown in Fig. 3 below each AFM image, indicate that the grain size of the investigated SiO_2 layer is around 60 nm. For a quantitative analysis of the surface roughness, the σ_{RMS} amplitude is plotted in Figure 4 as a function of the number of the irradiating pulse. We can see that the surface roughness amplitude decreases from 1.31 nm for the as-grown material to 1.07 nm for the 150-pulse-irradiated material. It is likely that laser-induced densification of SiO_2 and/or partial melting are the mechanisms responsible for this surface smoothing effect.

Downloaded from SPIE Digital Library on 03 Dec 2011 to 70.52.100.151. Terms of Use: http://spiedl.org/terms

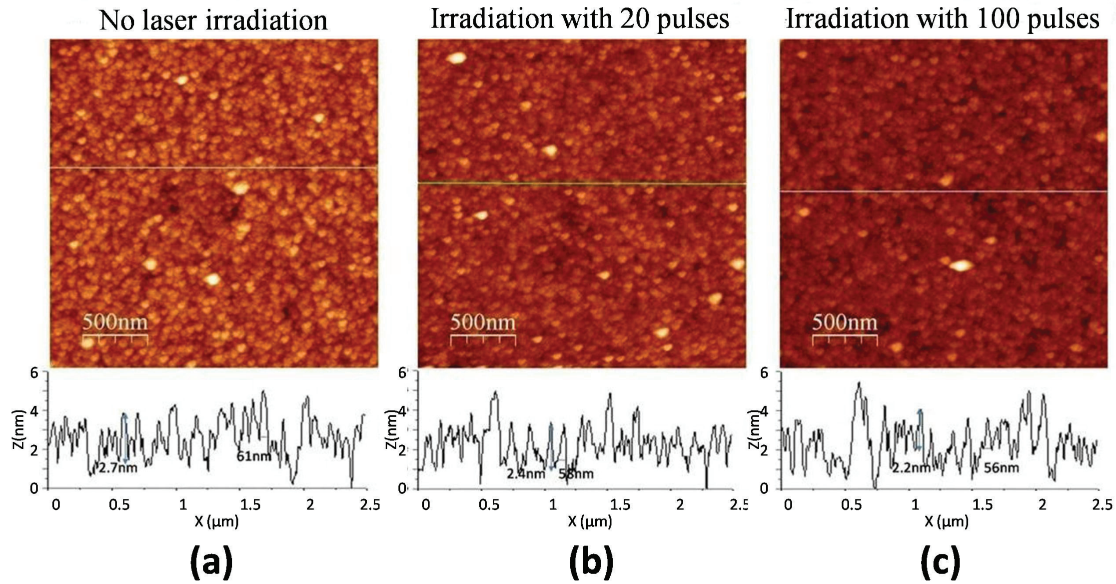

Figure 3. 2D AFM micrographs illustrating surface morphology of a 150 nm thick as-grown layer of SiO_2 (a), and following the irradiation with 20 (b) and 100 pulses (c) of the ArF laser at 76mJ/cm^2. In each case, the as-grown and laser irradiated samples were RTA for 2 min at 700° C.

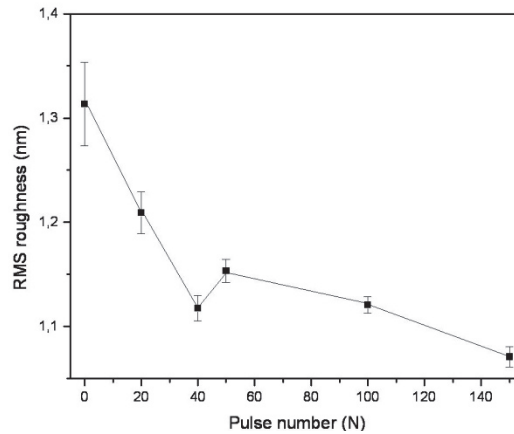

Figure 4. Roughness amplitude (σ_{RMS}) of the SiO_2 surface after ArF laser irradiation at 76 mJ/cm^2 with different pulse number and RTA for 2 min at 700° C.

Figure 5 illustrates surface morphology of InP after the SiO_2 layer was etched with the HF:H_2O solution. The site irradiated with 100 pulses seems smoother than that of the as-grown material. Also, fewer nanoparticles have been observed on the laser-irradiated sites than on the as-grown material. The average roughness (σ_{RMS}) of the laser-irradiated sites, shown in Figure 6, fluctuates around 0.4 nm. This figure also shows that the roughness uncertainty decreases with the number of pulses and gets closer to the one of a non-irradiated site. This demonstrates that SiO_2 layer protected InP surface from direct ArF laser irradiation, which is consistent with the absence of the laser-induced intermixing process observed in this case.

Downloaded from SPIE Digital Library on 03 Dec 2011 to 70.52.100.151. Terms of Use: http://spiedl.org/terms

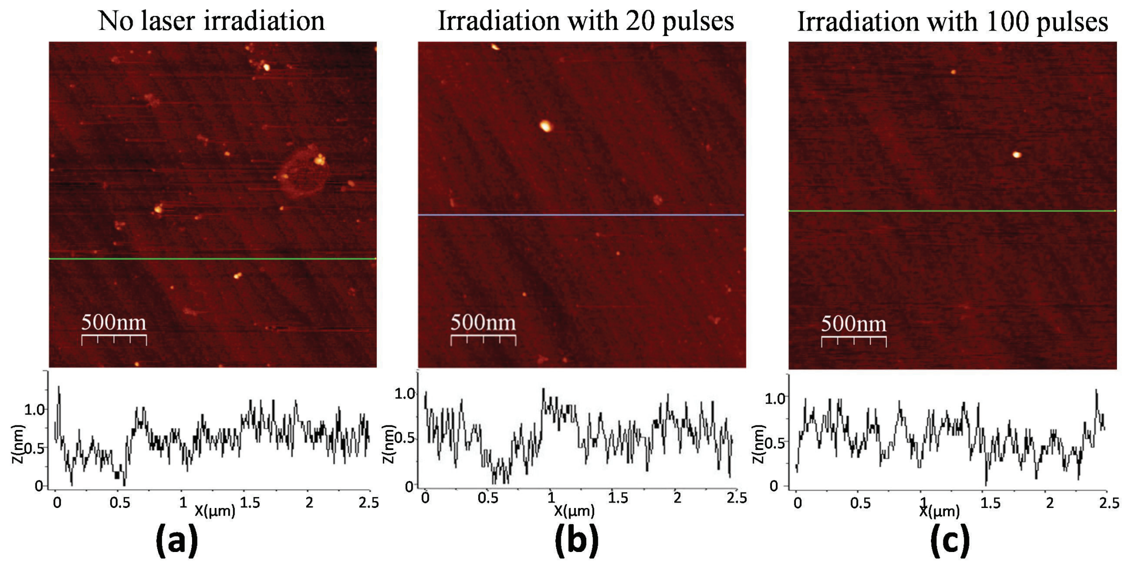

Figure 5. AFM micrographs of the InP surface after ArF laser irradiation with 76 mJ/cm^2 and RTA and after removing SiO_2 layer

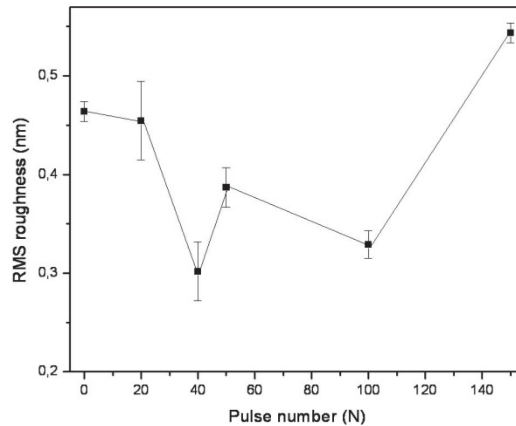

Figure 6. The RMS roughness of InP layer after ArF laser irradiation, RTA and after removing SiO_2 layer vs. pulse number for 76 mJ/cm^2

Figure 7 shows the 5 µm x 5 µm 2D and 3D AFM images of the InP surface revealed after the 150-nm-thick SiO_2 layer was ablated with 100 pulses of the ArF laser. The formation of a grating-like laser induced periodic surface structure (LIPSS)[24] is clearly observed in this region. The grating LIPSS period and height are around 1 µm and 10 nm, respectively. Figure 7 (a) also shows the presence of numerous 12 nm deep nano-holes on the processed surface. The roughness of this region is 2.11 nm, which compares to ~ 0.5 nm of the as-grown InP surface. We note that following the RTA step, the surface defects created during the ArF laser interaction with the InP layer induced, in this case, a 38 nm blueshift.

Downloaded from SPIE Digital Library on 03 Dec 2011 to 70.52.100.151. Terms of Use: http://spiedl.org/terms

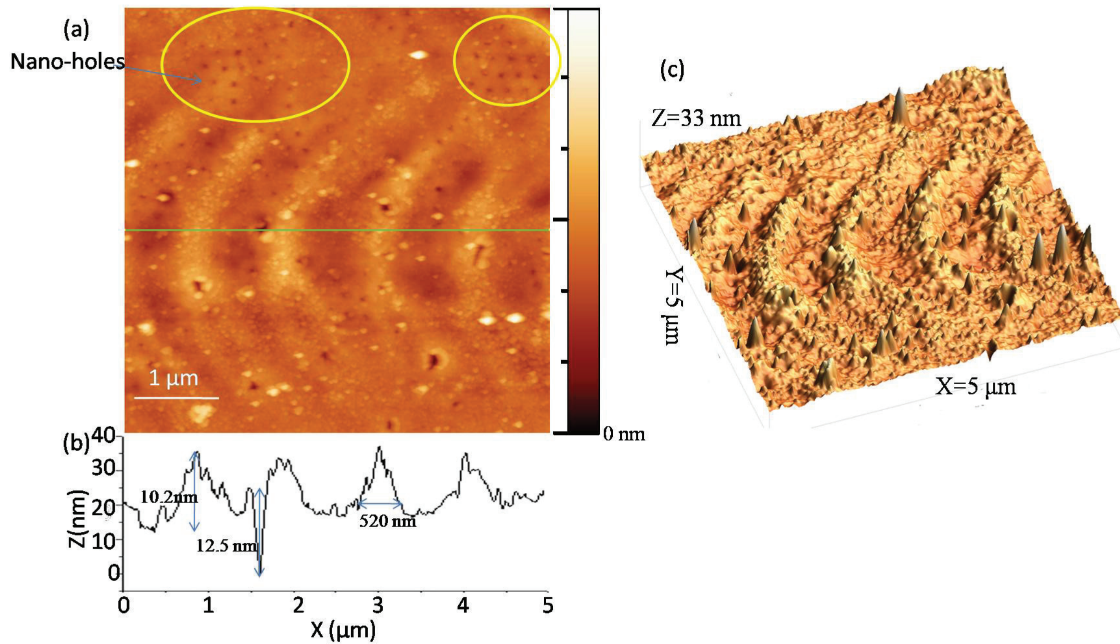

Figure 7. Surface morphology of the InP cap layer exposed to the ArF laser radiation in the region where SiO_2 was removed entirely.

3.2 KrF laser induced QWI on samples coated with SiO_2 layer

Figure 8 (a) shows PL maps and microscopic pictures of SiO_2 coated samples that were irradiated with the KrF laser at 156 mJ/cm^2 (Fig. 8a) and 128 mJ/cm^2 (Fig. 8b). It is evident that the 50 nm thick SiO_2 layer is ablated with 50 pulses at 156 mJ/cm^2. A partial removal of the 150 and 190 nm thick SiO_2 layers is observed following their irradiation with up to 200 pulses. A profilometric scan of the 150-pulse irradiated sample, initially coated with a 150 nm thick SiO_2 layer, revealed the formation of a 10 nm deep crater. This could be related to a partial ablation and/or densification of the laser-irradiated SiO_2 layer. In addition, numerous laser-induced microcracks have been observed for these samples. The microscopic pictures and PL maps of sites from samples coated 263 nm thick SiO_2, after KrF laser irradiation at 128 mJ/cm^2 and RTA, show no obvious laser ablation and blueshift for 50 and 100 pulses irradiated sites. At 200 pulses, the color of the SiO_2 layer changes significantly, which suggests that some structural changes take place in the laser irradiated SiO_2.

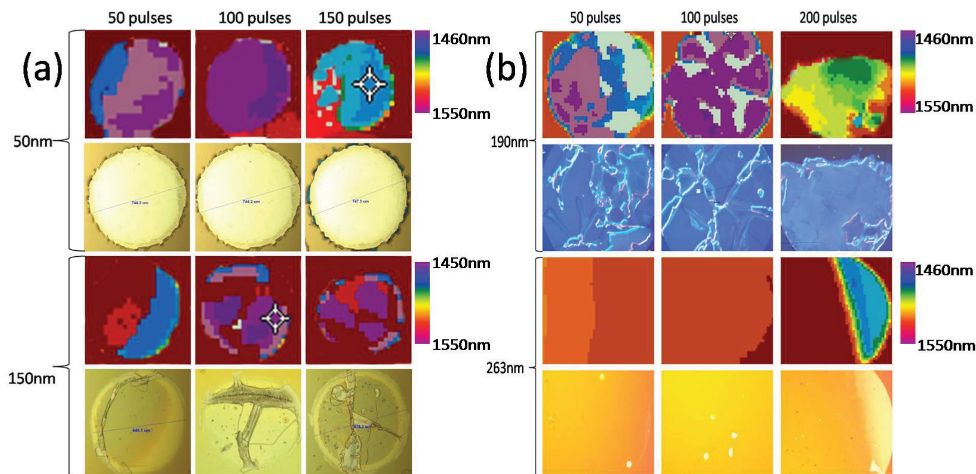

Figure 8. Room temperature PL maps and microscopic pictures of a series of spots on SiO_2 (50, 150, 190 and 263 nm thick) coated QW microstructures irradiated with the KrF laser at 156 mJ/cm^2 (a) and 128 mJ/cm^2 (b) and the indicated number of pulses.

Downloaded from SPIE Digital Library on 03 Dec 2011 to 70.52.100.151. Terms of Use: http://spiedl.org/terms

The results for samples coated with the 243-nm-thick SiO_2 layer, i.e., $d_{SiO2} \approx \lambda_{KrF}$, are summarized in Figure 9. It can be seen that the KrF laser irradiation with 124 mJ/cm^2 and RTA leads to blueshifts that, with the exception of the 200-pulse irradiated site, take place without the removal of the SiO_2 layer. The upper and lower numbers shown for each site in this figure indicate the laser pulse number and the average amplitude of blueshift, respectively. For example, it can be seen that the 8-pulse irradiated site has been blueshifted by 70 nm, and that the maximum blueshift of 74 nm is achieved after irradiation with 75 pulses. We note that a uniform blueshift of 59 nm has been achieved following the irradiation with only 5 laser pulses. Figure 10 summarizes the net blueshift vs. pulse number of both as-grown (uncoated) material and samples coated with a 243 nm thick SiO_2 layer following their irradiation with the KrF laser and the RTA step. The maximum blueshift for sample coated with 243 nm SiO_2 layer is less than that for the uncoated samples irradiated in an air environment. This may be due to the lower number of defects created on the surface of SiO_2 coated InP. It can be seen that for both samples, the blueshift increases with increasing the pulse number, then it has a tendency to saturate. At N>50 pulses, the blueshift for the uncoated sample decreases due to the obvious ablation effect which reduces the 'reservoir' of laser created defects.[7] However, for the sample coated with the 243 nm SiO_2 layer, the blueshift does not decrease, likely due to the protection against ablation that is provided by the SiO_2 layer.

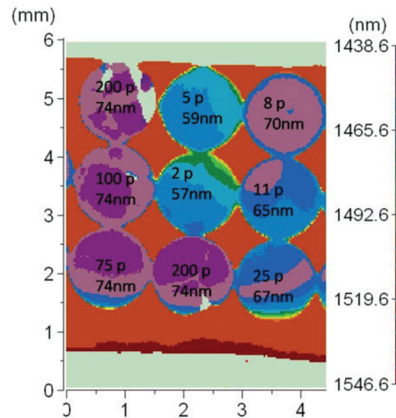

Figure 9. Room temperature PL map of an InP/InGaAs/InGaAsP QW microstructure after KrF laser irradiation and RTA. The pulse number and the blueshift amplitude are shown by the top and bottom numbers, respectively.

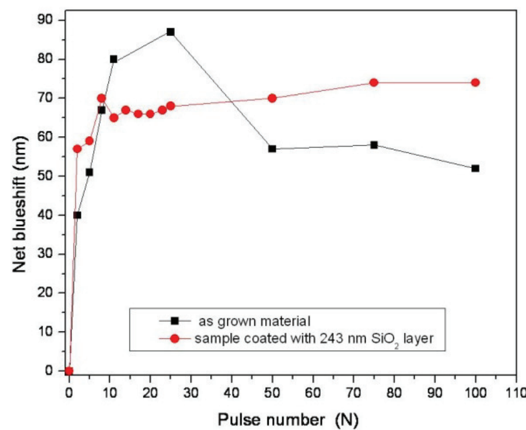

Figure 10. Net blueshift amplitude dependence on the pulse number of the KrF laser delivering 124 mJ/cm^2 and irradiating the surface of uncoated InP (square symbols) and SiO_2 (243 nm thick) coated InP cap (circle symbols). The results obtained after 2 min RTA at 700° C.

Table 1 shows the measured blueshift amplitude for a non-irradiated uncoated QW microstructure and for non-irradiated microstructures coated with d_{SiO2} = 50, 150, 190, 243 and 263 nm thick SiO_2 films. A 13 nm blueshift is observed for the microstructure coated with a 243 nm thick SiO_2, which is similar to the blueshift for the uncoated (d_{SiO2} = 0 nm) sample. These results demonstrate that the RTA-induced outdiffusion of In or P atoms from the InP/InGaAs/InGaAsP QW microstructure is negligible and, therefore, no efficient atomic intermixing can occur at the applied RTA temperature.[9]

Downloaded from SPIE Digital Library on 03 Dec 2011 to 70.52.100.151. Terms of Use: http://spiedl.org/terms

Table 1. Blueshift amplitude vs. thickness of the SiO_2 layer for non-irradiated QW microstructures.

SiO_2 layer thickness d_{SiO2} (nm)	0	50	150	190	243	263
Blueshift (nm)	13	11	10	11	13	13

The microscopic images of sites irradiated with 2, 25, 75 and 100 pulses of the KrF laser at 124 mJ/cm^2 are shown in Figure 11. The color change of the SiO_2 layer is likely related to the laser-induced densification and, consequently, change of the refractive index of this material.[25] The profilometry measurements have indicated that the overall thickness reduction of the irradiated SiO_2 layer does not exceed 10 nm.

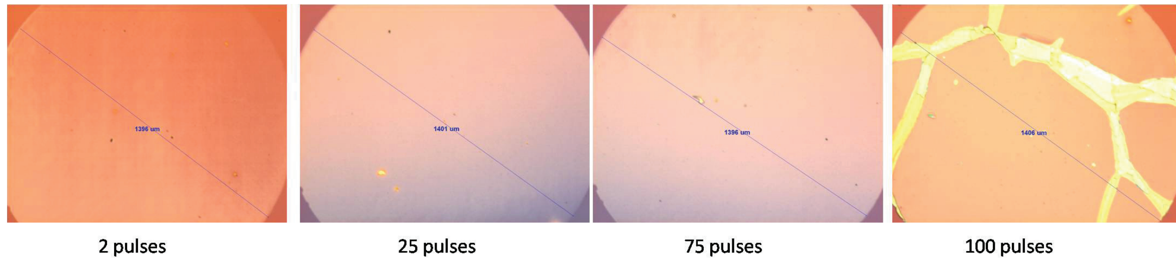

Figure 11. Microscopic images of KrF irradiated samples coated with a 243 nm SiO_2 layer and irradiated with the KrF laser at124 mJ/cm^2 (after RTA).

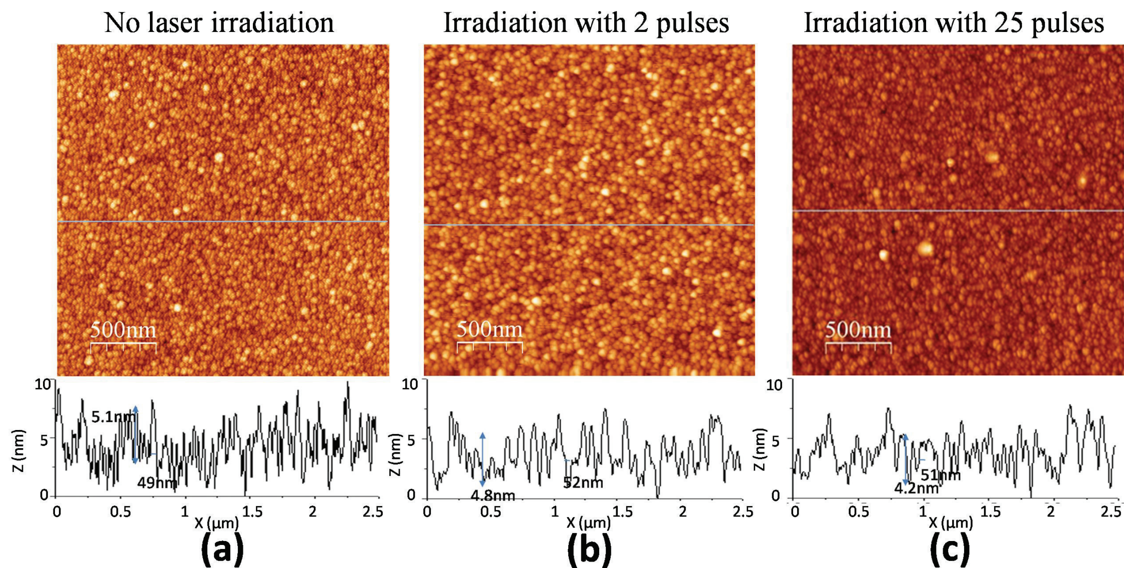

Figure 12. AFM micrographs of as-grown SiO_2 (a) and the SiO_2 layer irradiated with 2 pulses (b) and 25 pulses (c) of the KrF laser at 124 mJ/cm^2 (before RTA).

Figure 12 shows AFM micrographs of as-grown, 243 nm thick SiO_2 layer and the same thickness SiO_2 layer irradiated with 2 and 25 pulses of the KrF laser at 124 mJ/cm^2, before it was RTA. The grain structure of the material is well seen for both irradiated and non irradiated sites. The average grain size of this SiO_2 layer is around 50 nm, which is smaller than that of the 190 nm thick SiO_2 layer. The average grain height, measured by AFM, decreases from 5.22 nm (Fig. 12b) to 4.02 nm (Fig. 12c) as the pulse number increases up to 25 pulses.

The AFM images of the 243 nm thick SiO_2 layer, after it was RTA, are shown in Figure 13. The average grain height of the irradiated structures is reduced likely due to laser-induced melting.[20] This causes the roughness decreases by around

Downloaded from SPIE Digital Library on 03 Dec 2011 to 70.52.100.151. Terms of Use: http://spiedl.org/terms

0.1 nm after RTA as demonstrated in Figure 14. The initial roughness decrease when N<20 is due to laser heating and melting grain structure. Then it increases because of the nano-features creation at larger pulse number. Finally, it decreases again due to obvious laser material melting and partial removing of SiO_2 layer. The minimum achieved roughness is demonstrated on site irradiated with 20 pulses which gives 66 nm of blueshift.

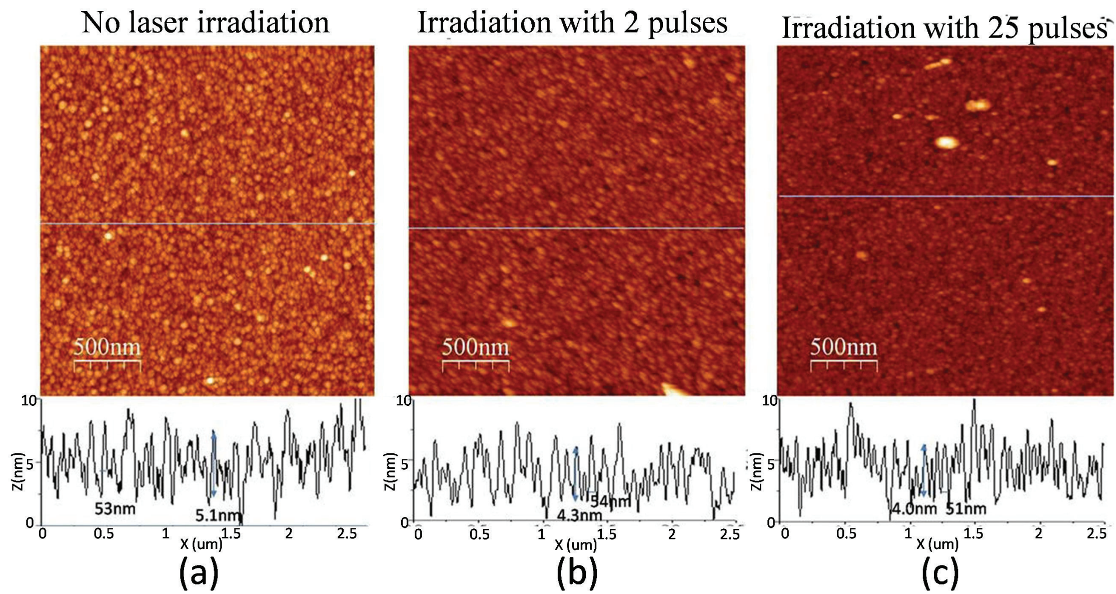

Figure 13. AFM micrographs of as-grown SiO_2 (a) and the SiO_2 layer irradiated with 2 pulses (b) and 25 pulses (c) of the KrF laser at 124 mJ/cm^2 (after RTA).

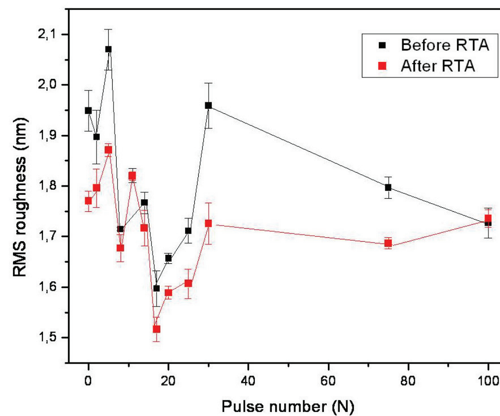

Figure 14. The RMS roughness of the SiO_2 layer after KrF laser irradiation at 124 mJ/cm^2 vs. pulse number before and after RTA.

The InP surface morphology of a non-irradiated InP and after the 2 and 25 pulse KrF laser irradiation (124 mJ/cm^2) of InP coated with the SiO_2 layer is shown in Figure 15. The results are shown after RTA and the removal of the SiO_2 layer. Numerous nano-holes created in InP can be seen for the 2 and, especially, for the 25-pulse irradiated surface. None of these nano-holes have been found on non irradiated sites, hence, the role of the KrF laser is evident in the formation of these nano-holes. It can be seen that the nano-hole depth increases from 2.5 nm to 3.3 nm and the width increases from 39 nm to 73 nm as the pulse number increases from 2 to 25 pulses. The density of nano-holes is also greatly increased for the 25 pulse irradiated site. We observed 8 nm deep, 83 nm wide nano-holes on sites irradiated with 100 pulses of the KrF laser (these results are not shown here). The formation of nano-holes leads to the increased average roughness of the irradiated surface, while the density of nano-holes saturation is observed at a large pulse number. The amplitude of

Downloaded from SPIE Digital Library on 03 Dec 2011 to 70.52.100.151. Terms of Use: http://spiedl.org/terms

blueshift dependence with pulse number follows the same behavior, as it can be seen in Figure 10. Therefore, it seems that the presence of nano-holes is somehow responsible for the intermixing process. The nano-holes may enhance P atom outdiffusion and create P vacancies, similarly to microcracks reported in QW irradiated with CW laser RTA.[10]

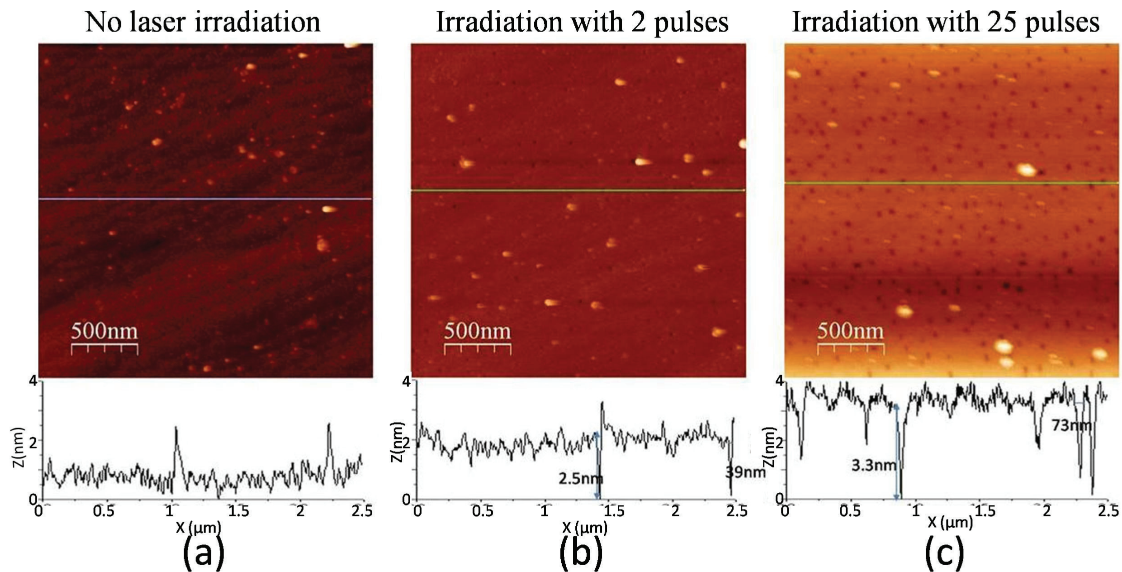

Figure 15. AFM surface morphology of a non-irradiated InP (a) and after the 2 pulse (b) and 25 pulse (c) KrF laser irradiation (124 mJ/cm^2) of InP coated with the SiO_2 layer. The results are shown after RTA and the removal of the SiO_2 layer.

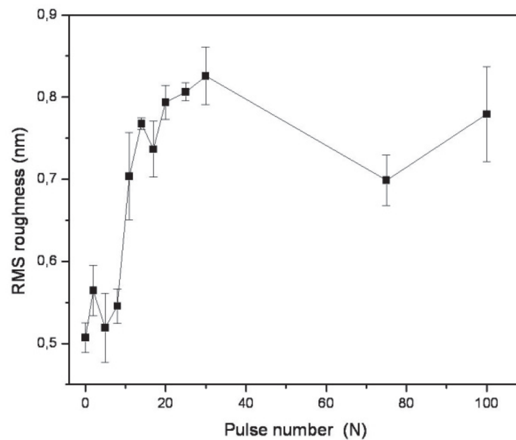

Figure 16. The RMS roughness of the InP layer irradiated with different pulses of the KrF at 124 mJ/cm^2, followed by the RTA step. The results are shown after the SiO_2 layer has been removed.

4. CONCLUSION

We have investigated morphology of SiO_2 and InP layers used for capping the InP/InGaAs/InGaAsP QW microstructure that were irradiated with the ArF and KrF excimer lasers. The SiO_2 roughness was found to decrease by increasing the pulse number of both lasers. We found out that the InP layer has a relatively smooth surface (σ_{RMS} ~0.4 nm) due to the protection provided by the SiO_2 layer during the excimer laser irradiation and high temperature RTA. For sample coated with 50 or 150 nm SiO_2 layer irradiated by the ArF laser, the blueshift is observed only in the region where the SiO_2 layer is ablated. The InP surface is altered by the ArF and KrF laser irradiation and results in the increased roughness. On the other hand, the maximum blueshift of 74 nm was achieved on sample coated with a 243 nm thick SiO_2 layer ($d_{SiO2} \approx \lambda_{KrF}$) showing a smooth surface (σ_{RMS} = 1.8 nm) after 75-pulse-radiation with the KrF laser at 124mJ/cm^2. A

Downloaded from SPIE Digital Library on 03 Dec 2011 to 70.52.100.151. Terms of Use: http://spiedl.org/terms

relatively large number of nano-holes have been observed in the InP layer irradiated with the KrF laser. The presence of these nano-holes coincides with the enhancement of the QWI process.

5. ACKNOWLEDGEMENT

This work was supported by the Merit Scholarship program for Foreign Students from the Fonds de Recherche sur la Nature et les Technologies (FQRNT) of Quebec (NL), the Natural Science and Engineering Research Council of Canada and the Canada Research Chair in Quantum Semiconductors program (JJD). The help from Abdelatif Jaouad, Guillaume Bertrand and Denis Pellé from the Université de Sherbrooke Centre de recherche en nanofabrication et en nanocaracterisation is greatly appreciated.

REFERENCES

[1] Li, E., [Semiconductor quantum wells intermixing], Gordon & Beach Science Publisher, Amsterdam, 8-11 (2000).
[2] Du, S., Fu, L., Tan, H., and Jagadish, C., "Investigations of impurity-free vacancy disordering in (Al) InGaAs (P)/InGaAs quantum wells," Semicond. Sci. Technol. 25, 055014 (2010).
[3] Laidig, W., Holonyak, N., Camras, M., Hess, K., Coleman, J., Dapkus, P., and Bardeen, J., "Disorder of an AlAs GaAs superlattice by impurity diffusion," Appl. Phys. Lett. 38(10), 776-778 (2009).
[4] Djie, H., Mei, T., Arokiaraj, J., Sookdhis, C., Yu, S., Ang, L., and Tang, X., "Experimental and theoretical analysis of argon plasma-enhanced quantum-well intermixing," IEEE J. Quantum Electron. 40(2), 166-174 (2004).
[5] Dubowski, J., "Laser-induced bandgap shifting for photonic device integration," US Patent #6,514,784 CA 2,331,567 (2002).
[6] Genest, J., Dubowski, J., and Aimez, V., "Suppressed intermixing in InAlGaAs/AlGaAs/GaAs and AlGaAs/GaAs quantum well heterostructures irradiated with a KrF excimer laser," Appl. Phys. A-Mater. 89(2), 423-426 (2007).
[7] Genest, J., Bearl, R., Aimez, V., and Dubowski, J., "ArF laser-based quantum well intermixing in InGaAs/InGaAsP heterostructures," Appl. Phys. Lett. 93, 071106 (2008).
[8] Teng, J., Dong, J., Chua, S., Lai, M., Foo, B., Thompson, D., Robinson, B., Lee, A., Hazell, J., and Sproule, I., "Controlled group V intermixing in InGaAsP quantum well structures and its application to the fabrication of two section tunable lasers," J. Appl. Phys. 92, 4330 (2002).
[9] Barik, S., Fu, L., Tan, H., and Jagadish, C., "Impurity-free disordering of InAs/ InP quantum dots," Appl. Phys. Lett. 90, 243114 (2007).
[10] Chia, C., Chua, S., Tripathy, S., and Dong, J., "Group-V intermixing in InAs/ InP quantum dots," Appl. Phys. Lett. 86, 051905 (2005).
[11] Bauerle, D., [Laser Processing and Chemistry], Springer-Verlag, Berlin Heidelberg, 307-330, (2000).
[12] Musaev, O., Kwon, O., Wrobel, J., Zhu, D., and Kruger, M., "Evolution of InP surfaces under low fluence pulsed UV irradiation," Appl. Surf. Sci. 254(18), 5803-5806 (2008).
[13] Bonse, J., Munz, M., and Sturm, H., "Scanning force microscopic investigations of the femtosecond laser pulse irradiation of indium phosphide in air," IEEE Trans. Nanotechnol. 3(3), 358-367 (2004).
[14] Messina, F., Cannas, M., and Boscaino, R., "Generation of defects in amorphous SiO_2 assisted by two-step absorption on impurity sites," J. Phys.: Condens. Matter 20, 275210 (2008).
[15] Lu, Y., Choi, W., Aoyagi, Y., Kinomura, A., and Fujii, K., "Controllable laser induced periodic structures at silico dioxide/silicon interface by excimer laser irradiation," J. Appl. Phys. 80 (12), 7052-7056 (2009).
[16] Yu, J. and Lu, Y., "Effects of rapid thermal annealing on ripple growth in excimer laser-irradiated silicon-dioxide/silicon substrates," Appl. Surf. Sci. 154, 670-674 (2000).
[17] Yu, J., Zhang, J., Boyd, I., and Lu, Y., "Excimer-laser-induced micropatterning of silicon dioxide on silicon substrates," Appl. Phys. A-Mater. 72(1), 35-39 (2001).
[18] Williams, K. and Muller, R., "Etch rates for micromachining processing," J. Microelectromech. S. 5(4), 256-269 (1996).
[19] Simpson, G., Sedin, D., and Rowlen, K., "Surface roughness by contact versus tapping mode atomic force microscopy," Langmuir 15(4), 1429-1434 (1999).

Downloaded from SPIE Digital Library on 03 Dec 2011 to 70.52.100.151. Terms of Use: http://spiedl.org/terms

[20] Dubowski, J., Poole, P., Sproule, G., Marshall, G., Moisa, S., Lacelle, C., and Buchanan, M., "Enhanced quantum-well photoluminescence in InGaAs/InGaAsP heterostructures following excimer-laser-assisted surface processing," Appl. Phys. A-Mater. 69, 299-303 (1999).
[21] Arai, K., Imai, H., Hosono, H., Abe, Y., and Imagawa, H., "Two photon processes in defect formation by excimer lasers in synthetic silica glass," Appl. Phys. Lett. 53(20), 1891-1893 (2009).
[22] Kim, Y. T., Kim, D. S., and Yoon, D. H., "PECVD SiO_2 and SiON films dependant on the rf bias power for low-loss silica waveguide," Thin Solid Films 475(1-2), 271-274 (2005).
[23] Wuu, D., Lo, W., Chiang, C., Lin, H., Chang, L., Horng, R., Huang, C., and Gao, Y., "Plasma-deposited silicon oxide barrier films on polyethersulfone substrates: temperature and thickness effects," Surf. Coat. Technol. 197(2-3), 253-259 (2005).
[24] Clark, S. and Emmony, D., "Ultraviolet-laser-induced periodic surface structures," Phys. Rev. B: Condens. Matter 40(4), 2031-2041 (1989).
[25] Mao, S., F, Q., Guizard, S., Mao, X., Russo, R., Petite, G., and Martin, P., "Dynamics of femtosecond laser interactions with dielectrics," Appl. Phys. A-Mater 79(7), 1695-1709 (2004).

Downloaded from SPIE Digital Library on 03 Dec 2011 to 70.52.100.151. Terms of Use: http://spiedl.org/terms